

q-AQUA: a Many-body CCSD(T) Water Potential, Including 4-body Interactions, Demonstrates the Quantum Nature of Water from Clusters to the Liquid Phase

Qi Yu,^{*,†} Chen Qu,^{*,‡} Paul L. Houston,^{*,¶} Riccardo Conte,^{*,§} Apurba Nandi,^{||} and
Joel M. Bowman^{*,||}

[†]*Department of Chemistry Yale University, New Haven, Connecticut 06520, U.S.A.*

[‡]*Independent researcher, Toronto, Ontario, Canada*

[¶]*Department of Chemistry and Chemical Biology, Cornell University, Ithaca, New York
14853, U.S.A. and Department of Chemistry and Biochemistry, Georgia Institute of
Technology, Atlanta, Georgia 30332, U.S.A*

[§]*Dipartimento di Chimica, Università degli Studi di Milano, via Golgi 19, 20133 Milano,
Italy*

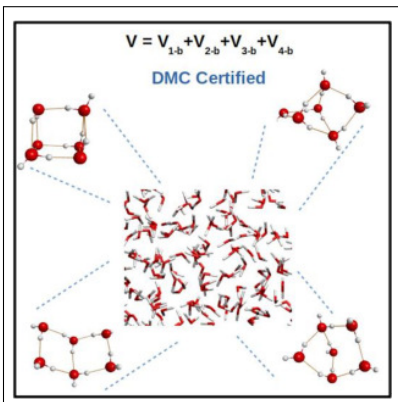
^{||}*Department of Chemistry and Cherry L. Emerson Center for Scientific Computation,
Emory University, Atlanta, Georgia 30322, U.S.A.*

E-mail: q.yu@yale.edu; szquchen@gmail.com; plh2@cornell.edu; riccardo.conte1@unimi.it;
jmbowma@emory.edu

Abstract

Many model potential energy surfaces (PESs) have been reported for water; however, none are strictly from “first principles”. Here we report such a potential, based on a many-body representation at the CCSD(T) level of theory up to the 4-body interaction. The new PES is benchmarked for the isomers of the water hexamer for dissociation energies, harmonic frequencies, and unrestricted diffusion Monte Carlo (DMC) calculations of the zero-point energies of the Prism, Book and Cage isomers. Dissociation energies of several isomers of the 20-mer agree well with recent benchmark energies. Exploratory DMC calculations on this cluster verify the robustness of the new PES for quantum simulations. The accuracy and speed of the new PES is demonstrated for standard condensed phase properties, i.e., the radial distribution function and the self-diffusion constant. Quantum effects are shown to be substantial for these observables and also needed to bring theory into excellent agreement with experiment.

TOC Graphic



Potential energy surfaces (PESs) are critical to our understanding of molecular interactions, their dynamics, and their structures. Among these surfaces, perhaps the most important are those that predict the behavior of life’s signature molecule, water. Ideally such a PES would employ the highest level of electronic structure theory and be developed for a complete many-body interaction. A major step in this direction was the CC-pol potential published in 2007.¹ This potential was based on fits to CCSD(T) interaction energies for rigid monomers at the 2-body(b) level of interaction and sophisticated treatments of long-range many-body induction effects. Since then numerous studies have examined the importance of 3-b, 4-b, and 5-b interactions, and the latest work² shows definitively that truncating at the 4-body level accounts for virtually all of the many-body interactions. So, it is clear now that an ideal approach for a water PES would include 2-b, 3-b and 4-b interactions for flexible monomers and using CCSD(T) level of theory. In addition, studies of structural and transport properties of water, ranging from clusters to condensed phase, should ideally be based on quantum simulations, which require a robust PES reaching to energies well beyond the zero-point energy. Finally, the PES should be invariant with respect to permutation of monomers, and each monomer should also be invariant with respect to interchange of the two H atoms.

We report such a PES here and apply it to a variety of important “stress tests” for clusters and the condensed phase. The form of this PES is based on the well-known, many-body expression for the total energy of N water monomers:

$$V(1, \dots, N) = \sum_{i=1}^N V_{1-b}(i) + \sum_{i>j}^N V_{2-b}(i, j) + \sum_{i>j>k}^N V_{3-b}(i, j, k) + \sum_{i>j>k>l}^N V_{4-b}(i, j, k, l) + \dots, \quad (1)$$

We indicate terms up to 4-b interactions explicitly because the potential in the present paper is truncated at this term. Each of these terms is obtained using a machine-learned fit to corresponding datasets of CCSD(T) interaction energies. Specifically, the fits are done using a basis of permutationally invariant polynomials (PIPs).³⁻⁵ This particular ML method has

been used by us previously in developing a water potential, denoted WHBB,⁶ and by Paesani and co-workers for the MB-pol water potential.^{7,8} These potentials are truncated at the *ab initio* level of 3-b interactions. Also, both use semi-empirical TTMn-F water potentials for higher-body interactions, however, in different ways. The WHBB PES uses TTM3-F⁹ while the MB-pol PES uses TTM4-F.¹⁰ There are significant differences in how these potentials are used in WHBB and MB-pol and these are described in detail in the Supporting Information (SI). Finally we note that there are numerous empirical water potentials, and we refer the reader to a recent review¹¹ of these along with the WHBB and MB-pol potentials.

The new fits reported here make use of new 2-b and 3-b datasets, which are at the CCSD(T) level and more extensive both in energy and range than the CCSD(T) 2- and 3-b datasets used for the MB-pol potential. In addition, a 4-b dataset, employed by us in a preliminary CCSD(T) PIP 4-b PES,¹² is extended and a new 4-b PIP fit is reported. Here we note the numbers of CCSD(T) energies in the datasets are 71,892, 45,332 and 3692 for the 2-, 3- and 4-b interactions, respectively. Additional details are given in the last section and in the SI. These new 2-, 3-, and 4-b PIP PESs together with the spectroscopically accurate Partridge and Schwenke¹³ water monomer (1-b) PES constitute the new PES. The new potential is denoted “q-AQUA”.

We now demonstrate the accuracy and robustness of q-AQUA for standard “stress” tests, namely the dissociation energies, harmonic frequencies, and diffusion Monte Carlo (DMC) calculations of zero-point energies of isomers of the water hexamer and the dissociation energies of several isomers of the 20-mer, for which benchmark values have recently been reported.¹⁴ We also report molecular dynamics (MD) and path integral molecular dynamics (PIMD) calculations for the radial distribution function (RDF) and MD and semi-quantum Ring Polymer MD (RPMD) calculations of the diffusion constant over a range of temperatures. Significant 4-b and quantum effects are found for these properties.

MB-pol is a highly successful water potential and so we present selected results using that potential as part of the assessment of q-AQUA. The first comparisons are for the 2-b

interaction with CCSD(T) benchmark calculations. For the 2-b interaction, attractive and repulsive cuts are presented in the SI where both q-AQUA and MB-pol are shown to be in excellent agreement with the CCSD(T) calculations.

Panels A and B of Fig. 1 show attractive and repulsive cuts, respectively, for the 3-b potential as one monomer is moved relative to the remaining dimer. The q-AQUA potential provides excellent agreement with CCSD(T) calculations throughout the 2–10 Å region. MB-pol is almost as accurate as q-AQUA for the attractive cut, but underestimates the repulsive 3-b potential in the 4–5.5 Å range and overestimates it considerably when the OO distance is less than 4 Å.

Panel C of Fig. 1 shows a 4-b potential cut as one monomer is moved with respect to the remaining trimer. The 4-b potential labeled “MB-pol” is the TTM4-F 4-b potential embedded in MB-pol. As seen, it is low compared to the CCSD(T) calculations in the range of about 3–5 Å, and is in strong disagreement with them below about 2.5 Å. The q-AQUA potential is in good agreement with CCSD(T) energies throughout the range shown. For moving one water dimer with respect to the other, panel D of Fig. 1 shows that, while the MB-pol has strong deviations from the CCSD(T) results below 2.5 Å, the q-AQUA potential is in good agreement with the CCSD(T) results throughout the range. One might expect that the TTM4-F 4-body potential embedded in MB-pol would be uniformly accurate in the long range, but this is not the case. This is shown in Fig. S9 of the SI, which plots the difference between CCSD(T)-F12 4-body energy and the MB-pol/TTM4-F 4-body energy against the maximum OO distance in the tetramer for all the configurations in our 4-body data set. The TTM4-F potential has large errors even when the OO distance is around 7 Å. The RMSE for TTM4-F, as compared to the CCSD(T)-F12 benchmark is 21.2 cm⁻¹, whereas the RMSE for the q-AQUA 4-b potential against the same benchmark is 7.2 cm⁻¹. Note that the average absolute value of the 4-b energy in the data set is 31.9 cm⁻¹, so an RMSE of 21.2 cm⁻¹ from TTM4-F is large. A correlation plot between the q-AQUA 4-b energies and the CCSD(T)-F12 ones is provided in Fig. S10 of the SI, where additional

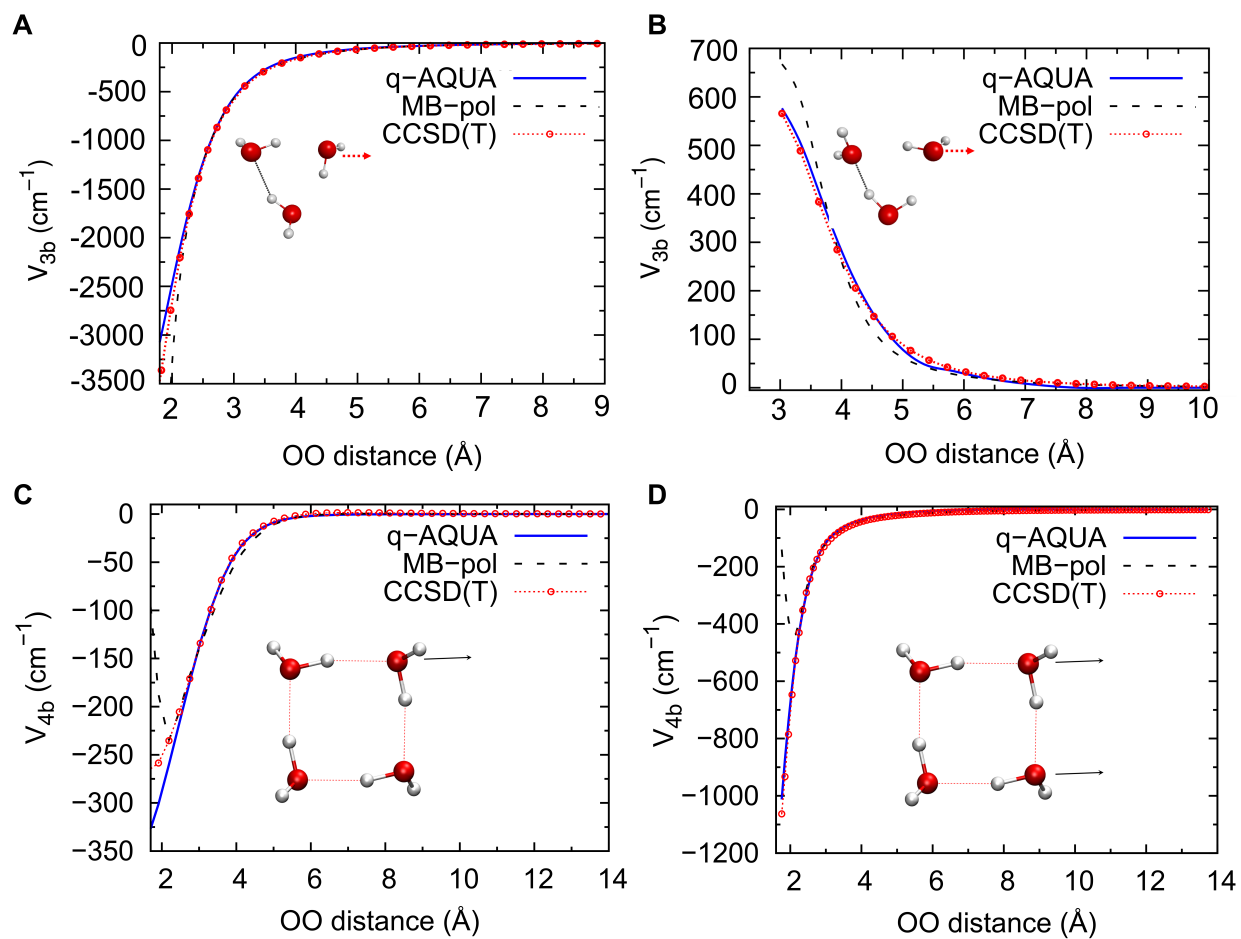


Figure 1: Comparison of the new 3-b fit and MB-pol with direct CCSD(T) energies for an attractive cut (A) and a repulsive cut (B). Comparison of the new 4-b fit and direct CCSD(T) energies for a monomer-trimer cut (C) and a dimer-dimer cut (D).

precision metrics and properties of the present 2-, 3-, and 4-b PIP potentials can be found.

Next, we present tests of the accuracy of q-AQUA against benchmark results for the water hexamer and the 20-mer. Table S1 in the SI provides results for each of the 8 hexamer isomers, comparing the dissociation energies and the 2-b, 3-b, and 4-b energies for the q-AQUA potential, the MB-pol potential and the CCSD(T)/CBS calculations.^{15,16} The mean absolute errors (MAEs) are lower in general for the q-AQUA potential, although both appear to be fairly accurate. These results are shown graphically in Fig. 2, where different levels of agreement with the CCSD(T) results are seen. The D_e results, particularly for the Ring, Boat1, and Boat2 isomers are more accurately predicted by q-AQUA than MB-pol, mostly because of differences in the 4-b contribution. Comparisons of the harmonic vibrational frequencies for four of the hexamer isomers are provided in Table S2 of the SI. As compared to the CCSD(T) benchmark calculation, q-AQUA and MB-pol are about equally good in predicting the frequencies of the Prism and Cage isomers, whereas q-AQUA does somewhat better than MB-pol on Book and Ring isomers.

The zero-point energies (ZPEs) of three hexamer isomers, Prism, Cage, and Book1, are calculated using the unrestricted diffusion Monte Carlo method.¹⁷⁻¹⁹ Details of these calculations are provided in the SI. The ZPEs of the three isomers (all referenced to the electronic energy of the Prism equilibrium structure) using the full q-AQUA potential and without the 4-b contribution are listed in Table 1, along with the statistical uncertainties. Note that due to a finite number of walkers and a finite step size, systematic errors on the absolute ZPE values exist, but early studies^{20,21} have shown that the energy differences between isomers are relatively insensitive to the number of walkers. The walker numbers used in this work are sufficient for a good estimate of the energy differences. As seen, the ZPE of the Cage is the lowest among the three isomers, by about 100 cm^{-1} and thus the Cage is predicted to be the lowest energy isomer at 0 K. This is in agreement with experiment^{22,23} and also the tentative conclusion of earlier DMC calculations using the WHBB PES.²¹ and even earlier calculations using rigid-body DMC.²² Further analysis of these DMC results and

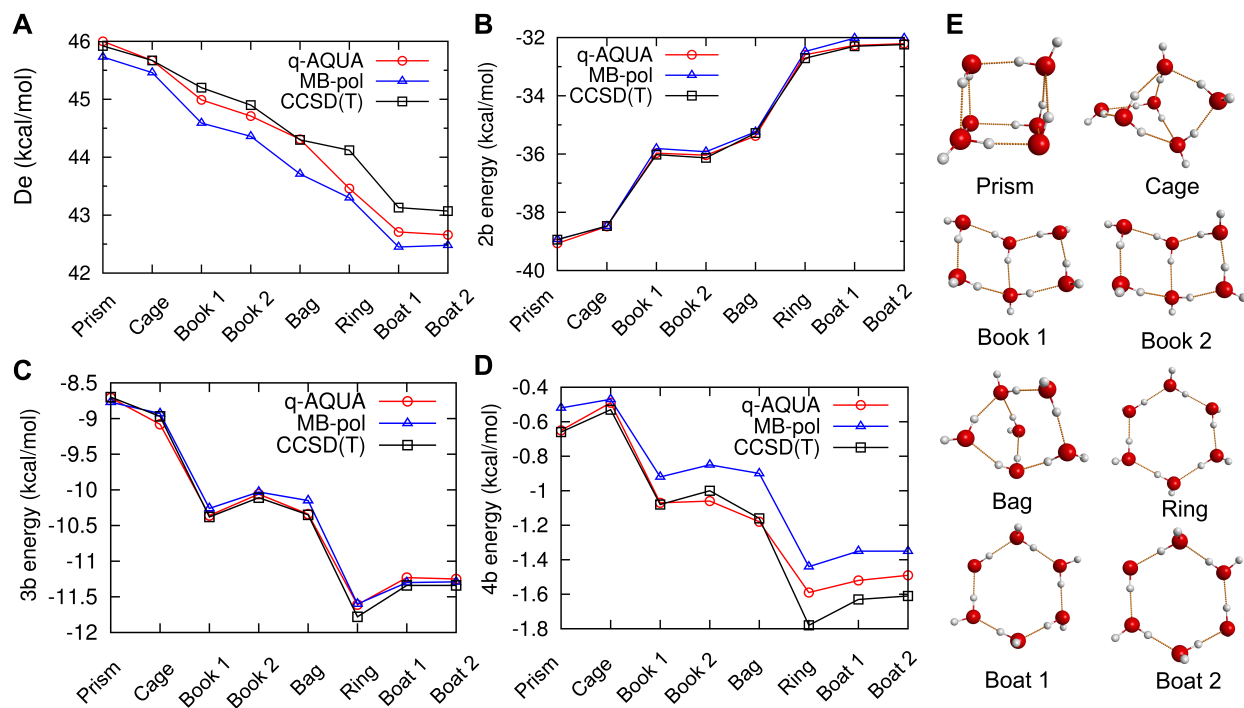


Figure 2: Binding energies (A), 2-body energies (B), 3-body energies (C) and 4-body energies (D) for water hexamer isomers from present fits, MB-pol and benchmark CCSD(T) calculations (taken from refs. 15 and 16). (E) Structures of water hexamer isomers.

also those for larger clusters will be the subject of a future paper.

As noted, the DMC calculations are unconstrained, unlike studies using MB-pol, where geometric constraints are applied.^{20,24} We have run unconstrained DMC calculations using MB-pol potential, and found many “holes”, i.e., configurations with unphysical very negative energies. By contrast, q-AQUA is “hole-free” when running unconstrained DMC, and this finding was further corroborated by DMC runs on the 20-mer which we discuss briefly next.

Table 1: Zero-point energies (in cm^{-1}) of three isomers of water hexamer from diffusion Monte Carlo calculations.

	With 4-b	Without 4-b
Prism	32647 ± 9	32598 ± 12
Cage	32553 ± 19	32465 ± 9
Book 1	32652 ± 12	32740 ± 16

Table 2: Binding energies (in kcal/mol) of three $(\text{H}_2\text{O})_{20}$ isomers.

Isomer	MP2/aV5Z	MP2/CBS	q-AQUA	MB-pol
A3	-202.1	$199.2 \pm 0.5^{\text{a}}$ ($-200.8 \pm 2.1^{\text{b}}$)	-199.8	-195.2
A2d	-202.1	n.a.	-201.7	-195.3
9	-201.5	n.a.	-200.5	-194.9

^a Ref. 14

^b CCSD(T)/CBS binding energy from Ref. 14

Table 2 shows the binding energies for three isomers of $(\text{H}_2\text{O})_{20}$ and compares the benchmark MP2/aV5Z and MP2/CBS calculations¹⁴ with the predictions of q-AQUA and MB-pol. The q-AQUA prediction for the A3 isomer is in good agreement with the MP2/CBS value, whereas the MB-pol value is more than 4 kcal/mol too low. Similarly, for the A2d and 9 isomers, the q-AQUA results are within one kcal/mol as compared to the available MP2/aV5Z results, while the MB-pol prediction is again too low by about 6–7 kcal/mol. It is interesting to note that without the 4-b interaction the binding energies from q-AQUA are close to those from MB-pol and so the present 4-b interaction is needed to close the gap with the benchmark results. Preliminary DMC calculations for the 20-mer have been performed successfully and this validates the robustness of the q-AQUA potential for a large cluster.

Finally we examine the q-AQUA potential for simulations of bulk water properties. Specifically, classical molecular dynamics (MD), path integral molecular dynamics (PIMD), and ring polymer molecular dynamics (RPMD)^{25,25,26} were used to calculate both static and dynamic properties of liquid water. All the MD simulations were performed with the i-PI software,²⁷ and more computational details about calculations are provided in the SI.

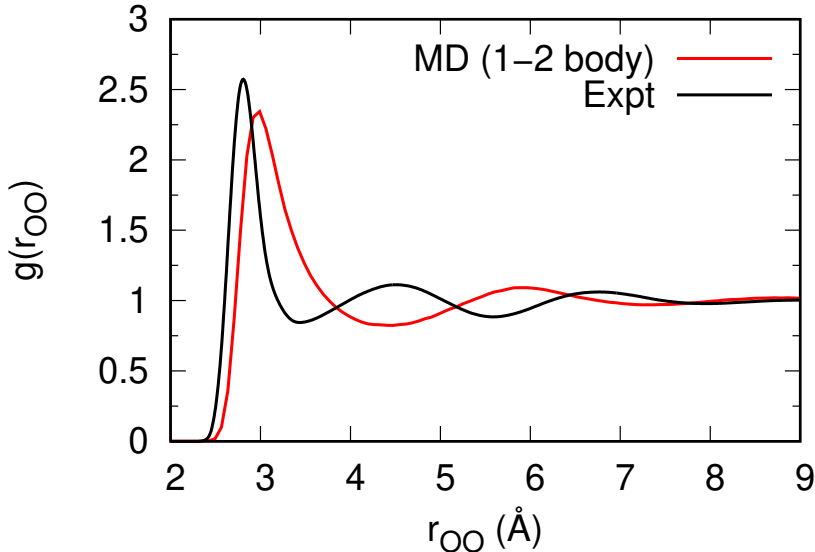


Figure 3: OO radial distribution function from classical MD simulations at 298 K using reduced q-AQUA potential up to and including the 2-b interaction. The experimental data are from Ref. 28

Fig. 3 shows the OO radial distribution function obtained from classical molecular dynamics simulations at 298 K with only 1-b and 2-b interactions included. As seen, the simulated OO radial distribution deviates significantly from the experimental measurement. The inclusion of 1-b and 2-b interactions cannot sufficiently describe the water interactions in the condensed phase. Panels A and B of Fig. 4 show the q-AQUA results for MD and PIMD simulations of the OO radial distribution function over a range of temperatures for 1-, 2-, 3-b and 1-4-body interactions compared to experiment (data taken from Refs. 28,29). Although the classical MD prediction agrees substantially with the position of the peaks in the distribution, it is noteworthy that the amplitudes of the peaks do not agree well. For

the quantum calculations, the agreement is substantially better; see also Fig. S14 and S15. These plots do lead to the conclusion that for this property the 4-b interaction is not needed to obtain the graphical level of agreement seen. Fig. S14 in the SI shows this RDF using q-AQUA truncated at the 2-b, 3-b and 4-b levels. As seen there, truncating at the 2-b level does not give an accurate result. Interestingly the peaks move to shorter OO distances in going from the 2-b, to 3-b and finally 4-b level of truncation. This implies the presence of an effective additional attraction in going to the higher level of n -body interaction. Figure S14 also demonstrates that for these simulations, the many-body expansion converges rapidly. The differences between the 1-2-body, 1-3-body, and 1-4-body results decrease progressively to a few percent, as does the difference between these results and the experiment. Figure S16 compares the radial distribution functions for the OO, OH, and HH distributions to experimental results.

Next consider the self-diffusion constant as a function of temperature obtained with q-AQUA using MD and RPMD calculations. The results are given in Table 3. As seen, MD gets the trend correctly but is low compared to the experiment, whereas RPMD succeeds in coming close to the experiment. The extent of quantum effects in the self-diffusion constant has been discussed previously in the context of the approximate and largely empirical q-TIP4P/F potential.²⁶ This effect is estimated at 1.15 using that potential, which is less than the factor of around 1.5 in the present calculations. With respect to this difference, we note the statement in ref. 26 about “competing quantum effects” and also where it was concluded that “...in our q-TIP4P/F model, these two effects nearly cancel one another, leading to a comparatively small net quantum effect on the diffusion coefficient.” Evidently the current water potential, which is the first one including an ab initio 4-b interaction there is less cancellation of competing effects. The orientational relaxation time at 298 K is also given and, as seen, is in much better agreement when quantum RPMD as compared to the classical MD.

Thus, for both the radial distribution function and especially the diffusion constant,

quantum effects are significant for liquid water. And it is clear that q-AQUA provides accurate results when coupled with quantum dynamics. Space does not permit a detailed discussion of these studies, but we simply note that the present calculations find significant quantum effects in both, and especially for the diffusion constant the magnitude seen here is consistent with recent results using an empirical water potential.³⁰ For the first time the effect of the 4-b has been shown to decrease the diffusion constant somewhat. This implies that overall the 4-b is an added attraction which retards the diffusion, a result that seems quite reasonable to us.

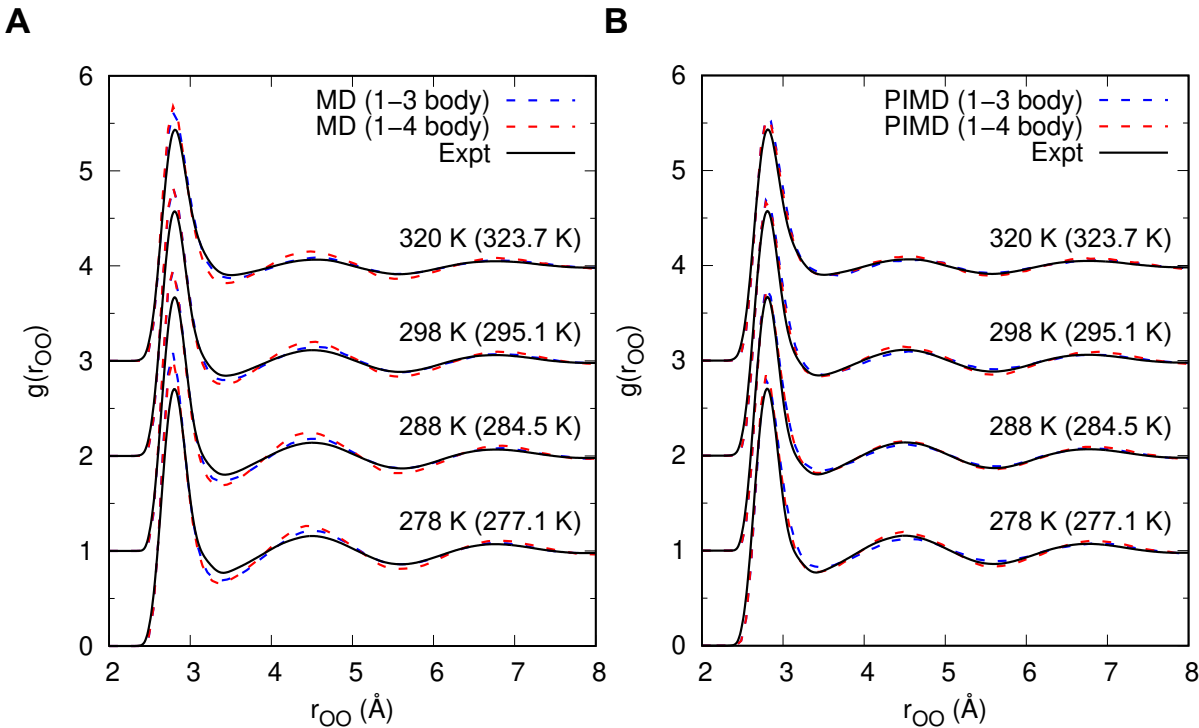


Figure 4: OO radial distribution function from classical (A) and path integral (B) molecular dynamics simulations at different temperatures. The blue dashed lines are from reduced q-AQUA potential up to and including the 3-b interaction. The red dashed lines are from the full q-AQUA potential up to and including the 4-b interaction. The experimental data are taken from Ref. 28,29

Finally, we present some timing results for q-AQUA. For the dynamics of 256 water molecules, Table S5 in the SI provides information for the time required for each of the n -body steps and for the total, with and without periodic boundary conditions (PBC), for one

Table 3: Dynamical properties of liquid water from classical and quantum simulations with q-AQUA potential

Self-diffusion coefficient, $D, (\text{\AA}^2/\text{ps})$			
Temperature (K)	Classical	RPMD	Expt. ^a
278	0.080 ± 0.016	0.130 ± 0.015	0.131
288	0.102 ± 0.017	0.177 ± 0.015	0.177
298	0.145 ± 0.012	0.226 ± 0.020	0.230
320	0.248 ± 0.011	0.331 ± 0.016	0.360
Orientational relaxation time, $\tau_2, (\text{ps})$			
Temperature (K)	Classical	RPMD	Expt. ^b
298	3.2 ± 0.1	2.4 ± 0.2	2.5

^a from Ref. 31 and 32

^b from Ref. 33

2.4 GHz Intel Xeon core or eight using OpenMP, and for both the energy alone and for the energy and gradients. The number of calculations required for each n -body component is also shown. The energy cost for the combined n -body components is about 2 s without PBC and about 4.5 s with PBC. The cost to get all gradients is about 2.3–2.4 times the cost of the energy due to the efficiency provided by the implementation of reverse derivatives.⁵ Using 8 cores rather than one speeds up the process by a factor of 6.2–6.6. The most expensive part of the process is the calculation of the 4-body interactions, of which 268,304 or 115,922 are evaluated with or without PBC, respectively. For a single 200000-step MD trajectory with 256 water molecules under PBC, it takes around 40 hours when 15 CPU cores are used. For some calculations, it may be possible to truncate the MBE after the 3-b interactions, in which case the times are cut by more than a factor of two.

In summary, q-AQUA is a new water potential that is fully *ab initio*-based and robust for quantum simulations. An interesting aspect of this potential is that it can be used very efficiently at lower-levels of the many-body expansion and higher-body interactions can be investigated via approximate methods such as perturbation theory. This opens up a new line of investigation that can be studied in the future.

COMPUTATIONAL DETAILS

The q-AQUA potential is composed of separate PIP fits for each of the n -body interactions with $n=1-4$. The 1-b fit is the spectroscopically accurate water monomer PES calculated by Partridge and Schwenke.¹³ The 2-b through 4-b fits are purified, compacted fits (2b is not purified) to new, expanded datasets containing CCSD(T) energies for 71892, 45332, and 3692 geometries, respectively. The processes for purification and compaction as well as for the addition of reverse derivatives to provide gradients are described in the SI, along with additional details for each of the fits.

Briefly, the 2-b fit used a basis set of PIPs with 7th-order, 42 symmetry; it has an RMS error of 25 cm^{-1} . The data set was limited to OO distances in the range from 2 to 8 Å, whereas the long-range 2-b interaction was accounted for by a dipole-dipole interaction using a high-level dipole moment surface³⁴ and a smooth switching function.

The new PIP 3-b PES that is a significant advance over the earlier one used in the WHBB PES. First, 45332 electronic energies are calculated at the CCSD(T)-F12a/aVTZ level of theory with BSSE correction included. This new 3-b data set extends over a broader energy range and covers a larger maximum OO distance range from 2.1 to 10.0 Å. We then divided the new 3-b data set into two separate sets: one with maximum OO distance in the range from 2.0 to 7.0 Å with 42145 structures, and another with maximum OO distance in the range from 5.0 to 9.5 Å, with 15282 structures. The short-range data set was fit using 4th-order 222111-symmetry PIPs of Morse variables, while the long-range data set is fit using 3rd-order 222111-symmetry PIPs of inverse internuclear distances. The fitting RMS errors for the short-range and long-range data sets are 9 cm^{-1} and 11 cm^{-1} , respectively. A smooth switching function is used to join the two fits.

We recently reported the first CCSD(T)-based PES for the twelve-atom 4-b interaction,¹² and the 4-b used in q-AQUA is an improved version of that PES. Here we just briefly describe the improvement. First, the size of the data set is expanded to 3692 from the original 2119 in order to cover more tetramer configurations. Second, we grouped the polynomials with the

same coefficient into one polynomial, so that the data set does not have to be replicated 24 times for the fit, and the number of polynomials is greatly reduced. Lastly, the polynomial basis is augmented with a selection of 4th-order PIPs. The final basis set consists of 200 (grouped) polynomials and the RMS fitting error is 7.2 cm^{-1} . (For comparison, the RMS is 10.2 cm^{-1} if the original basis is used to fit the expanded data set.)

Details of the hexamer results, the Diffusion Monte Carlo calculations and the MD and PIMD simulations are found in the SI.

ASSOCIATED CONTENT

Supporting Information available

- Discussion of differences between the q-AQUA, MB-pol, and WHBB potentials
- Description of three methods to optimize the basis set of polynomials used in calculating n -body potential energy surfaces: Purification, Pruning, and Analytic Gradients
- Details concerning each of the 2-body, 3-body, and 4-body potential energy surfaces
- Further details concerning the hexamer results, including predictions of the q-AQUA and MB-pol potentials and comparison to the CCSD(T)/CBS calculations for the harmonic frequencies for four of the water hexamers
- Details concerning the Diffusion Monte Carlo (DMC) calculations
- Details concerning the Molecular Dynamics (MD) simulations
- A compressed file containing Fortran programs for all of the multibody potentials. Data sets associated with these PES fits will be made available at <https://github.com/jmbowma/QM-22>.

AUTHOR INFORMATION

Corresponding Authors

*E-mail: q.yu@yale.edu

*E-mail: szquchen@gmail.com

*E-mail: PLH2@cornell.edu

*E-mail: riccardo.conte1@unimi.it

*E-mail: jmbowma@emory.edu

ORCID

Qi Yu: 0000-0002-2030-0671

Chen Qu: 0000-0001-8889-4851

Paul L. Houston: 0000-0003-2566-9539

Riccardo Conte: 0000-0003-3026-3875

Apurba Nandi: 0000-0002-6191-5584

Joel M. Bowman: 0000-0001-9692-2672

Notes

The authors declare no competing financial interest

ACKNOWLEDGMENTS

JMB thanks the ARO, DURIP grant (W911NF-14-1-0471), for funding a computer cluster where most of the calculations were performed and current financial support from NASA (80NSSC20K0360). QY thanks Professor Sharon Hammes-Schiffer and National Science

Foundation (Grant No. CHE-1954348) for support. RC thanks Università degli Studi di Milano ("PSR, Azione A Linea 2 - Fondi Giovani Ricercatori") for support.

References

- (1) Bukowski, R.; Szalewicz, K.; Groenenboom, G. C.; van der Avoird, A. Predictions of the Properties of Water from First Principles. *Science* **2007**, *315*, 1249.
- (2) Heindel, J. P.; Xantheas, S. S. The Many-Body Expansion for Aqueous Systems Revisited: I. Water–Water Interactions. *J. Chem. Theory Comput.* **2020**, *16*, 6843–6855.
- (3) Braams, B. J.; Bowman, J. M. Permutationally Invariant Potential Energy Surfaces in High Dimensionality. *Int. Rev. Phys. Chem.* **2009**, *28*, 577–606.
- (4) Conte, R.; Qu, C.; Houston, P. L.; Bowman, J. M. Efficient Generation of Permutationally Invariant Potential Energy Surfaces for Large Molecules. *J. Chem. Theory Comput.* **2020**, *16*, 3264–3272.
- (5) Houston, P. L.; Qu, C.; Nandi, A.; Conte, R.; Yu, Q.; Bowman, J. M. Permutationally Invariant Polynomial Regression for Energies and Gradients, Using Reverse Differentiation, Achieves Orders of Magnitude Speed-up with High Precision Compared to Other Machine Learning Methods. *J. Chem. Phys.* **2022**, *156*, 044120.
- (6) Wang, Y. M.; Shepler, B. C.; Braams, B. J.; Bowman, J. M. Full-Dimensional, Ab Initio Potential Energy and Dipole Moment Surfaces for Water. *J. Chem. Phys.* **2009**, *131*, 054511.
- (7) Babin, V.; Leforestier, C.; Paesani, F. Development of a “First Principles” Water Potential with Flexible Monomers: Dimer Potential Energy Surface, VRT Spectrum, and Second Virial Coefficient. *J. Chem. Theory Comput.* **2013**, *9*, 5395.

- (8) Babin, V.; Medders, G. R.; Paesani, F. Development of a “First Principles” Water Potential with Flexible Monomers. II: Trimer Potential Energy Surface, Third Virial Coefficient, and Small Clusters. *J. Chem. Theory Comput.* **2014**, *10*, 1599.
- (9) Fanourgakis, G. S.; Xantheas, S. S. Development of Transferable Interaction Potentials for Water. V. Extension of the Flexible, Polarizable, Thole-Type Model Potential (TTM3-F, v. 3.0) to Describe the Vibrational Spectra of Water Clusters and Liquid Water. *J. Chem. Phys.* **2008**, *128*, 074506.
- (10) Burnham, C. J.; Anick, D. J.; Mankoo, P. K.; Reiter, G. F. The Vibrational Proton Potential in Bulk Liquid Water and Ice. *J. Chem. Phys.* **2008**, *128*, 154519.
- (11) Cisneros, G. A.; Wikfeldt, K. T.; Ojamäe, L.; Lu, J.; Xu, Y.; Torabifard, H.; Bartók, A. P.; Csányi, G.; Molinero, V.; Paesani, F. Modeling Molecular Interactions in Water: From Pairwise to Many-Body Potential Energy Functions. *Chem. Rev.* **2016**, *116*, 7501–7528.
- (12) Nandi, A.; Qu, C.; Houston, P. L.; Conte, R.; Yu, Q.; Bowman, J. M. A CCSD(T)-Based 4-Body Potential for Water. *J. Phys. Chem. Lett.* **2021**, *12*, 10318–10324.
- (13) Partridge, H.; Schwenke, D. W. The Determination of an Accurate Isotope Dependent Potential Energy Surface for Water from Extensive Ab Initio Calculations and Experimental Data. *J. Chem. Phys.* **1997**, *106*, 4618.
- (14) Heindel, J. P.; Herman, K. M.; Aprà, E.; Xantheas, S. S. Guest–Host Interactions in Clathrate Hydrates: Benchmark MP2 and CCSD(T)/CBS Binding Energies of CH₄, CO₂, and H₂S in (H₂O)₂₀ Cages. *J. Phys. Chem. Lett.* **2021**, *12*, 7574–7582.
- (15) Bates, D. M.; Tschumper, G. S. CCSD(T) Complete Basis Set Limit Relative Energies for Low-Lying Water Hexamer Structures. *J. Phys. Chem. A* **2009**, *113*, 3555–3559.

- (16) Reddy, S. K.; Straight, S. C.; Bajaj, P.; Huy Pham, C.; Riera, M.; Moberg, D. R.; Morales, M. A.; Knight, C.; Götz, A. W.; Paesani, F. On the Accuracy of the MB-pol Many-body Potential for Water: Interaction Energies, Vibrational Frequencies, and Classical Thermodynamic and Dynamical Properties from Clusters to Liquid water and Ice. *J. Chem. Phys.* **2016**, *145*, 194504.
- (17) Anderson, J. B. A Random-walk Simulation of the Schrödinger Equation: H_3^+ . *J. Chem. Phys.* **1975**, *63*, 1499–1503.
- (18) Anderson, J. B. Quantum Chemistry by Random Walk. $\text{H } ^2P$, $\text{H}_3^+ D_{3h} ^1A'_1$, $\text{H}_2 ^3\Sigma_u^+$, $\text{H}_4 ^1\Sigma_g^+$, $\text{Be } ^1S$. *J. Chem. Phys.* **1976**, *65*, 4121–4127.
- (19) Kosztin, I.; Faber, B.; Schulten, K. Introduction to the Diffusion Monte Carlo Method. *Am. J. Phys.* **1996**, *64*, 633–644.
- (20) Mallory, J. D.; Brown, S. E.; Mandelshtam, V. A. Assessing the Performance of the Diffusion Monte Carlo Method As Applied to the Water Monomer, Dimer, and Hexamer. *J. Phys. Chem. A* **2015**, *119*, 6504–6515.
- (21) Wang, Y. M.; Babin, V.; Bowman, J. M.; Paesani, F. The Water Hexamer: Cage, Prism, or Both. Full Dimensional Quantum Simulations Say Both. *J. Am. Chem. Soc.* **2012**, *134*, 11116.
- (22) Liu, K.; Brown, M. G.; Carter, C.; Saykally, R. J.; Gregory, J. K.; Clary, D. C. Characterization of a Cage Form of the Water Hexamer. *Nature* **1996**, *381*, 501–503.
- (23) Pérez, C.; Muckle, M. T.; Zaleski, D. P.; Seifert, N. A.; Temelso, B.; Shields, G. C.; Kisiel, Z.; Pate, B. H. Structures of Cage, Prism, and Book Isomers of Water Hexamer from Broadband Rotational Spectroscopy. *Science* **2012**, *336*, 897–901.
- (24) Mallory, J. D.; Mandelshtam, V. A. Diffusion Monte Carlo Studies of MB-pol $(\text{H}_2\text{O})_{2-6}$

- and $(\text{D}_2\text{O})_{2-6}$ Clusters: Structures and Binding Energies. *J. Chem. Phys.* **2016**, *145*, 064308.
- (25) Miller, T. F.; Manolopoulos, D. E. Quantum Diffusion in Liquid Water from Ring Polymer Molecular Dynamics. *J. Chem. Phys.* **2005**, *123*, 154504.
- (26) Habershon, S.; Markland, T. E.; Manolopoulos, D. E. Competing Quantum Effects in the Dynamics of aFlexible Water Model. *J. Chem. Phys.* **2009**, *131*, 024501.
- (27) Kapil, V.; Rossi, M.; Marsalek, O.; Petraglia, R.; Litman, Y.; Spura, T.; Cheng, B.; Cuzzocrea, A.; Meißner, R. H.; Wilkins, D. M. et al. i-PI 2.0: A Universal Force Engine for Advanced Molecular Simulations. *Comput. Phys. Commun.* **2019**, *236*, 214–223.
- (28) Skinner, L. B.; Huang, C.; Schlesinger, D.; Pettersson, L. G. M.; Nilsson, A.; Benmore, C. J. Benchmark Oxygen-oxygen Pair-distribution Function of Ambient Water from X-ray Diffraction Measurements with a Wide Q-range. *J. Chem. Phys.* **2013**, *138*, 074506.
- (29) Skinner, L. B.; Benmore, C. J.; Neufeind, J. C.; Parise, J. B. The Structure of Water around the Compressibility Minimum. *J. Chem. Phys.* **2014**, *141*.
- (30) Eltareb, A.; Lopez, G. E.; Giovambattista, N. Nuclear Quantum Effects on the Thermodynamic, Structural, and Dynamical Properties of Water. *Phys. Chem. Chem. Phys.* **2021**, *23*, 6914–6928.
- (31) Mills, R. Self-diffusion in Normal and Heavy Water in the Range 1-45°. *J. Phys. Chem.* **1973**, *77*, 685–688.
- (32) Holz, M.; Heil, S. R.; Sacco, A. Temperature-dependent Self-diffusion Coefficients of Water and Six Selected Molecular Liquids for Calibration in Accurate ^1H NMR PFG Measurements. *Phys. Chem. Chem. Phys.* **2000**, *2*, 4740–4742.

- (33) Rezus, Y. L. A.; Bakker, H. J. On the Orientational Relaxation of HDO in Liquid Water. *J. Chem. Phys.* **2005**, *123*, 114502.
- (34) Lodi, L.; Tennyson, J.; Polyansky, O. L. A Global, High Accuracy Ab Initio Dipole Moment Surface for the Electronic Ground State of the Water Molecule. *J. Chem. Phys.* **2011**, *135*, 034113.